

Elastic properties of the rare-earth dititanates $R_2\text{Ti}_2\text{O}_7$ ($R = \text{Tb}$, Dy , and Ho)

Y. Nakanishi,* T. Kumagai, and M. Yoshizawa

Department of Materials Science and Engineering, Iwate University Morioka 020-8551, Japan

K. Matsuhira and S. Takagi

Department of Electronics, Faculty of Engineering, Kyushu Institute of Technology, Kitakyushu 804-8550, Japan

Z. Hiroi

Institute for Solid State Physics, University of Tokyo, Chiba 277-8581, Japan

(Received 3 March 2011; revised manuscript received 28 March 2011; published 31 May 2011; publisher error corrected 19 September 2011)

We have performed ultrasonic measurements on the α -pyrochlore spin compounds $R_2\text{Ti}_2\text{O}_7$, $R = \text{Tb}$, Dy , and Ho . A distinct dip appears around 80 K, especially in transverse modes $(C_{11} - C_{12})/2$ and C_{44} as a function of temperature in $\text{Dy}_2\text{Ti}_2\text{O}_7$ and $\text{Ho}_2\text{Ti}_2\text{O}_7$ compounds. This anomaly may correspond to a structural change detected by the temperature dependence of the permittivity and of the loss-angle tangent. No distinct anomaly was observed at lower temperatures in $\text{Dy}_2\text{Ti}_2\text{O}_7$ and $\text{Ho}_2\text{Ti}_2\text{O}_7$ compounds. On the other hand, a pronounced elastic softening toward low temperatures was observed in the temperature dependence of the principal elastic constants C_{11} , $(C_{11} - C_{12})/2$, and C_{44} in $\text{Tb}_2\text{Ti}_2\text{O}_7$. A detailed discussion of the highly distinct behavior among three compounds is given in terms of the magnitude of a splitting energy between the ground state and the excited one formed by the crystal-field effect. It seems that geometrically structural frustration prohibits the formation of a long-range quadrupolar ordering as well as a magnetic one, even if the coupling constant between quadrupolar moments is rather large enough in $\text{Tb}_2\text{Ti}_2\text{O}_7$ at low temperatures.

DOI: [10.1103/PhysRevB.83.184434](https://doi.org/10.1103/PhysRevB.83.184434)

PACS number(s): 75.50.Lk, 72.50.+b, 75.80.+q

I. INTRODUCTION

Pyrochlore rare-earth titanates with the general formula $R_2\text{Ti}_2\text{O}_7$ (where $R = \text{rare earth}$) exhibit a rich variety of interesting magnetic phenomena due to their characteristic crystal structure.¹ They crystallize in a cubic structure (space group $Fd\bar{3}m$) and consist of two kinds of three-dimensional networks individually formed of corner-sharing tetrahedra of R_2 or Ti_4 .² Antiferromagnetically coupled spins residing on the network of corner-sharing tetrahedra result in the phenomenon of geometrical frustration. They are frustrated not only for the nearest-neighbor antiferromagnetic interaction but also for the ferromagnetic interaction under a uniaxial crystal anisotropy. Pyrochlore rare-earth titanates are a well-known example of a three-dimensional geometrically frustrated system.³ Depending on the nature of the magnetic rare-earth ion R in these compounds, their ground states can exhibit a wide variety of phenomena such as long-range magnetic order, spin ice physics, and a highly correlated quantum disordered state known as a collective paramagnet or spin liquid. For $\text{Ho}_2\text{Ti}_2\text{O}_7$ and $\text{Dy}_2\text{Ti}_2\text{O}_7$, ferromagnetic interactions with strong uniaxial anisotropy lead to the frustrated state “spin ice.”^{4–11} On the other hand, for antiferromagnetic Tb titanates, exchange and dipolar interactions have the same order of magnitude, and they compete also with the anisotropy energy.^{12–14} It is thus expected that the effect of frustration possibly appears in a different form from those of the other titanates.

Let us briefly review the low-temperature property of those titanates.^{4–11} For $\text{Dy}_2\text{Ti}_2\text{O}_7$ and $\text{Ho}_2\text{Ti}_2\text{O}_7$, the Weiss temperatures are estimated from the magnetic susceptibility measurement to be about 0.5 and 1.9 K, respectively. The Dy^{3+} and Ho^{3+} ions possess a strong Ising anisotropy along the local $\langle 111 \rangle$ axis. Indeed, the magnetization curves for the three principal directions of an applied magnetic field can

be described by a model containing purely Ising anisotropy. An important point to emphasize is that a macroscopically degenerate ground state is possibly formed at low temperatures derived from the multiplicity of the possible spin configurations. By analogy with proton disorder in ice, I_h , the spin configuration with two spins pointing inward and two spins pointing outward for each tetrahedron corresponds to the ice rule for these compounds, so-called spin ices.¹⁵ In fact, $\text{Dy}_2\text{Ti}_2\text{O}_7$ shows a residual entropy of 1.68 J/mol K, which is numerically in agreement with Pauling’s entropy for water ice, $R(1/2)\ln(3/2)$.^{10,11}

On the other hand, for $\text{Tb}_2\text{Ti}_2\text{O}_7$, the Weiss temperature is estimated from the magnetic susceptibility measurement to be about 19 K, indicating that nearest-neighbor interaction between the Tb^{3+} ions is antiferromagnetic.^{12–14} A spin liquid state can be possibly realized for large classical spins derived from Tb^{3+} , which persists down to 70 mK at least, well below the energy scale of the antiferromagnetic interactions estimated by the Weiss temperature. A single ion ground state of Tb^{3+} is a degenerate doublet, yielding an Ising-like character for the Tb^{3+} spins, with a reduced magnetic moment of $5\mu_B$, which is well below the expected free ion value of $9\mu_B$. The magnetization curves of $\text{Tb}_2\text{Ti}_2\text{O}_7$ show a rather small anisotropy as compared with that of spin ice systems $\text{Dy}_2\text{Ti}_2\text{O}_7$ and $\text{Ho}_2\text{Ti}_2\text{O}_7$. It is considered that quantum fluctuations within the ground state and between the ground state and first excited one play a crucial role in forming the intriguing spin liquid state. A significant contrast in anisotropy in the magnetization curves originates from the energy separation between the ground state and first excited one in these compounds.

Ultrasonic measurements are particularly suited to explore ground-state properties of rare-earth compounds. A

quadrupolar susceptibility deduced from the ultrasonic experiment provides valuable and significant information to determine the $4f$ ground state of the R ion split by the crystalline electric field (CEF) effect. The quadrupolar susceptibility, as the elastic constant, measures the diagonal (Curie terms) and off-diagonal (Van Vleck terms) quadrupolar matrix elements. The quadrupolar response of the $4f$ electronic ground state split by the CEF effect causes a characteristic anomaly in the temperature dependence of the elastic constants due to the Curie terms.

In this paper, we report on the elastic properties of single-crystal pyrochlore rare-earth titanates $R_2\text{Ti}_2\text{O}_7$ ($R = \text{Dy}, \text{Ho},$ and Tb), investigated by ultrasonic measurements. We will discuss the ground-state properties and the origin of the giant magnetostriction in $\text{Tb}_2\text{Ti}_2\text{O}_7$, in comparison with its absence in $\text{Dy}_2\text{Ti}_2\text{O}_7$ and $\text{Ho}_2\text{Ti}_2\text{O}_7$. The present results indicate that low-temperature properties of these compounds are governed by a low-lying energy level, in particular for $\text{Tb}_2\text{Ti}_2\text{O}_7$.

II. EXPERIMENT

Single crystals have been grown by the floating-zone method using an infrared furnace equipped with four halogen lamps and elliptical mirrors. The crystals were grown under O_2 gas flow to avoid oxygen deficiency. The typical growth rate was 4 mm/h. The obtained single crystals were translucent yellow. A specimen used for the present measurement was cut into a rectangular shape with two axes along the $\langle 100 \rangle$ and $\langle 011 \rangle$ directions. The thicknesses along $\langle 100 \rangle$ and $\langle 011 \rangle$ are 2.0 and 1.8 mm for $\text{Dy}_2\text{Ti}_2\text{O}_7$, 2.0 and 1.6 mm for $\text{Ho}_2\text{Ti}_2\text{O}_7$, and 2.0 and 1.6 mm for $\text{Tb}_2\text{Ti}_2\text{O}_7$, respectively. The sound velocity was measured with an ultrasonic apparatus based on the phase comparison method in a magnetic field up to 12 T generated by a superconducting magnet. We used piezoelectric plates of LiNbO_3 for the transducer of the ultrasonic wave generator and detector with frequencies from 5 to 30 MHz. The transducers were glued on the parallel planes of the sample with the elastic polymer Thiokol. The absolute velocity was obtained by measuring the delay time for the sequence of ultrasonic echoes. The elastic constant $C = \rho v^2$ can be estimated from the sound velocity v and the density ρ of the crystal; here $\rho = 6.87 \text{ g/cm}^3$ for $\text{Dy}_2\text{Ti}_2\text{O}_7$, $\rho = 6.94 \text{ g/cm}^3$ for $\text{Ho}_2\text{Ti}_2\text{O}_7$, and $\rho = 6.70 \text{ g/cm}^3$ for $\text{Tb}_2\text{Ti}_2\text{O}_7$.

III. QUADRUPOLEAR MOMENT-STRAIN INTERACTION

The characteristic elastic softening toward low temperatures, observed in the temperature dependence of the elastic constants, is a quantum phenomenon. The elastic softening of a localized f electron system can usually be understood as the quadrupolar response of the system to an external strain associated with the sound wave. The volume strain $\varepsilon_B = \varepsilon_{xx} + \varepsilon_{yy} + \varepsilon_{zz}$ with Γ_1 symmetry associated with the bulk modulus $C_B = (C_{11} + 2C_{12})/3$ couples to the Coulomb multipole moment $O_B = O_4^0 + 5O_4^4$. A softening in C_B is a characteristic phenomenon for the valence fluctuation system such as SmB_6 , for example. C_B increases with decreasing temperature due to the anharmonicity of the lattice vibration in the compound with stable $4f$ electrons and even in the Kondo compounds. The elastic strain $\varepsilon_v = \varepsilon_{xx} - \varepsilon_{yy}$ and

$\varepsilon_u = (2\varepsilon_{zz} - \varepsilon_{xx} - \varepsilon_{yy})/\sqrt{3}$ associated with the transverse $(C_{11} - C_{12})/2$ mode couples to the quadrupolar moment $O_2^2 = J_{xx} - J_{yy}$ and $O_2^0 = (2J_z^2 - J_x^2 - J_y^2)/\sqrt{3}$, respectively, with Γ_3 symmetry. On the other hand, the elastic strain ε_{xy} associated with the transverse C_{44} mode couples to the quadrupolar moment O_{xy} with Γ_5 symmetry. The lowest order term of this perturbation can be described by¹⁶⁻²³

$$H_{qs} = \sum_i g_\Gamma O_\Gamma(i) \varepsilon_\Gamma. \quad (1)$$

Here, $O_\Gamma(i)$ is the equivalent quadrupolar operator at the i th R site and g_Γ (where Γ denotes the irreducible representation of the point group, i.e., Γ_3 and Γ_5) is the coupling constant. The scattering of the conduction electrons by the electric quadrupolar moments of $4f$ electrons leads to a quadrupolar interaction such as the RKKY mechanism. This means that the quadrupolar moment $O_\Gamma(i)$ of the i th R site couples to the moment of the other sites by way of the conduction electrons with the same mechanism as the RKKY interaction. This intersite quadrupolar interaction can be described by

$$H_{qq} = \sum_i g'_\Gamma \langle O_\Gamma \rangle O_\Gamma(i). \quad (2)$$

Here, g'_Γ is the quadrupolar coupling constant and $\langle O_\Gamma \rangle$ is the mean field of the quadrupolar moment. The temperature dependence of the symmetric elastic constant C_Γ is described as

$$C_\Gamma(T) = C_\Gamma^{(0)}(T) - \frac{N g_\Gamma^2 \chi_\Gamma^{(s)}(T)}{1 - g'_\Gamma \chi_\Gamma^{(s)}(T)}. \quad (3)$$

Here, N denotes the number of R ions per unit volume, and $C_\Gamma^{(0)}$ and $\chi_\Gamma^{(s)}(T)$ denote the background without the quadrupolar-strain interaction and the quadrupolar susceptibility, respectively.

IV. EXPERIMENTAL RESULTS

Figure 1 shows the temperature dependence of the elastic constants of $\text{Dy}_2\text{Ti}_2\text{O}_7$. C_{11} was measured by longitudinal ultrasonic waves with frequencies of 10 or 30 MHz propagating along the $\langle 100 \rangle$ axis with polarization along the $\langle 100 \rangle$ axis. $(C_{11} - C_{12})/2$ and C_{44} were measured by transverse ultrasonic waves with frequencies of 5 or 15 MHz propagating along the $\langle 110 \rangle$ axis with polarization along the $\langle 1-10 \rangle$ axis and along the $\langle 100 \rangle$ axis with polarization along the $\langle 010 \rangle$ axis, respectively. The absolute values of each elastic constant and calculated bulk modulus $C_B = (C_{11} + 2C_{12})/3$ and the Poisson ratio $\gamma_p = C_{12}/(C_{11} + C_{12})$ from C_{11} and $(C_{11} - C_{12})/2$ at both 77 and 4.2 K of $\text{Dy}_2\text{Ti}_2\text{O}_7$ are listed in Table I. The $\text{Dy}_2\text{Ti}_2\text{O}_7$ data exhibit roughly normal behavior at high temperatures: a stiffening with decreasing temperature. However, it is seen that a slight dip was observed in $(C_{11} - C_{12})/2$ and C_{44} around 80 K. They all stay almost constant below 40 K. Figure 2 shows the temperature dependence of the elastic constants of $\text{Ho}_2\text{Ti}_2\text{O}_7$. The absolute values of each elastic constant and calculated bulk modulus $C_B = (C_{11} + 2C_{12})/3$ and the Poisson ratio $\gamma_p = C_{12}/(C_{11} + C_{12})$ from C_{11} and $(C_{11} - C_{12})/2$ at both 77 and 4.2 K of $\text{Ho}_2\text{Ti}_2\text{O}_7$ are listed in Table II. The overall behavior is almost the same as that

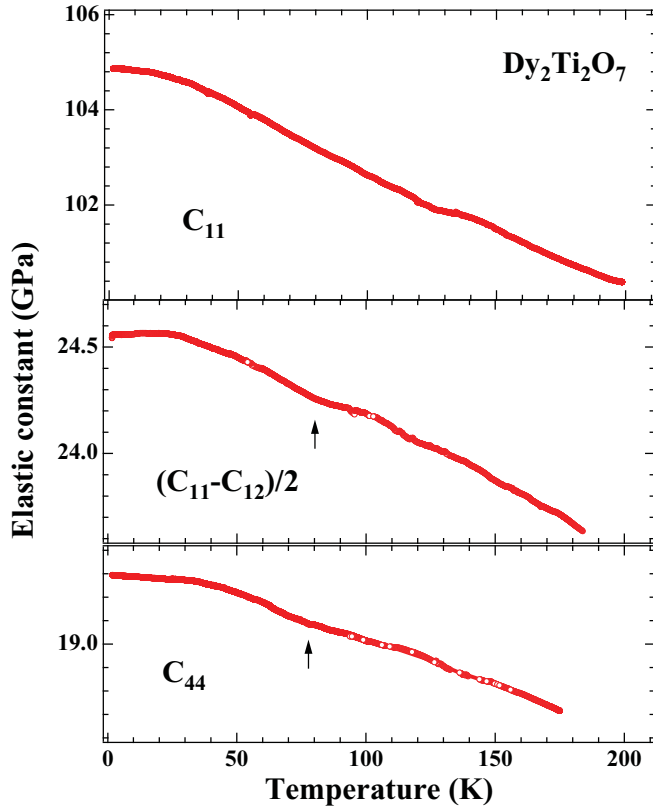


FIG. 1. (Color online) Temperature dependence of the elastic constants C_{11} , $(C_{11} - C_{12})/2$, and C_{44} of $\text{Dy}_2\text{Ti}_2\text{O}_7$. The anomaly is indicated by the arrows.

of $\text{Dy}_2\text{Ti}_2\text{O}_7$. However, a more distinct dip was observed in $(C_{11} - C_{12})/2$ and C_{44} around 80 K. Similar to that of $\text{Dy}_2\text{Ti}_2\text{O}_7$, a flat behavior below 40 K is observed in all principal elastic constants.

Mamsurova *et al.*, reported the dielectric properties of $\text{Dy}_2\text{Ti}_2\text{O}_7$ and $\text{Ho}_2\text{Ti}_2\text{O}_7$.²⁴ A clear anomaly was observed around 80 K and a smaller anomaly was observed around 30 K in the temperature dependence of the permittivity $\varepsilon(T)$ and the loss-angle tangent, $\tan\delta(T)$, as will be discussed in detail below.

By contrast, $\text{Tb}_2\text{Ti}_2\text{O}_7$ exhibits markedly different behavior in the temperature dependence of elastic constants as shown in Fig. 3. One observes strong softening effects for principal elastic constants, which are due to the magnetoelastic coupling of the sound waves to the $4f$ electronic charge distribution

TABLE I. The absolute values of each elastic constant and bulk modulus $C_B = (C_{11} + 2C_{12})/3$ and the Poisson ratio $\gamma = C_{12}/(C_{11} + C_{12})$ of $\text{Dy}_2\text{Ti}_2\text{O}_7$ at both 77 and 4.2 K.

Mode	Elastic constants	
	at 4.2 k	at 77 k
C_{11}	104.9 GPa	103.3 GPa
$(C_{11} - 2C_{12})/2$	24.6 GPa	24.3 GPa
C_{44}	19.3 GPa	19.1 GPa
$C_B = (C_{11} + 2C_{12})/3$	72.1 GPa	70.9 GPa
$\gamma_p = C_{12}/(C_{11} + C_{12})$	0.347	0.346

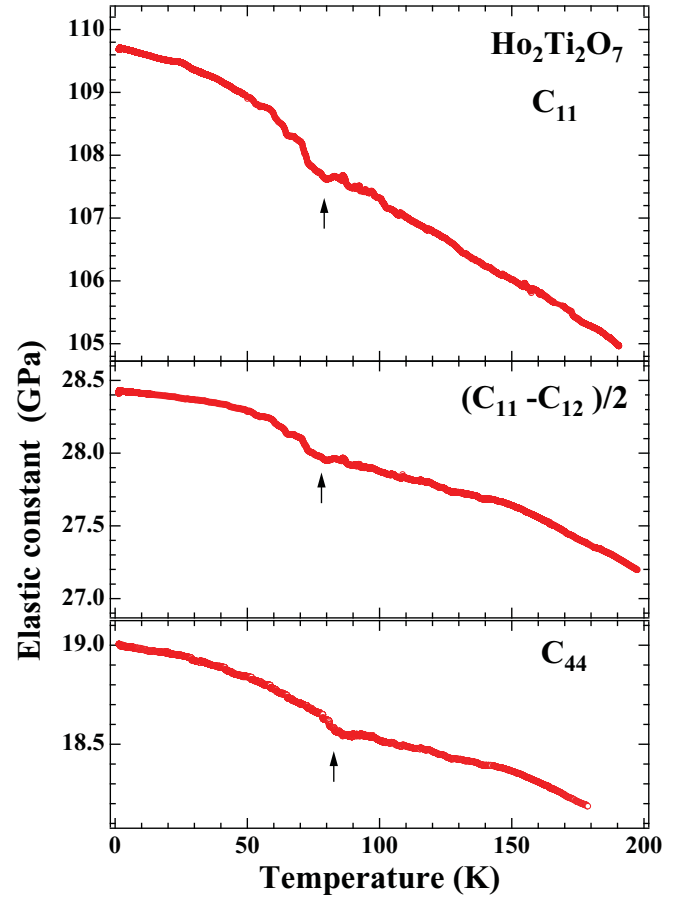


FIG. 2. (Color online) Temperature dependence of the elastic constants C_{11} , $(C_{11} - C_{12})/2$, and C_{44} of $\text{Ho}_2\text{Ti}_2\text{O}_7$. The anomaly is indicated by the arrows.

of the Tb^{3+} ions. The softening for C_{11} , $(C_{11} - C_{12})/2$, and C_{44} amounts to 10%, 15%, and 14%, respectively. The absolute values of each elastic constant and calculated bulk modulus $C_B = (C_{11} + 2C_{12})/3$ and the Poisson ratio $\gamma_p = C_{12}/(C_{11} + C_{12})$ from C_{11} and $(C_{11} - C_{12})/2$ at both 77 and 4.2 K of $\text{Tb}_2\text{Ti}_2\text{O}_7$ are listed in Table III. Figure 4 shows the temperature dependence of C_{11} at low temperatures under the selected magnetic fields along the $\langle 100 \rangle$ axis, offset for clarity in ascending order from bottom to top. The softening below 30 K becomes suppressed gradually with increasing magnetic field. Figure 5 shows the low-temperature part of C_{11} as a function of temperature under selected magnetic fields

TABLE II. The absolute values of each elastic constant and bulk modulus $C_B = (C_{11} + 2C_{12})/3$ and the Poisson ratio $\gamma_p = C_{12}/(C_{11} + C_{12})$ of $\text{Ho}_2\text{Ti}_2\text{O}_7$ at both 77 and 4.2 K.

Mode	Elastic constants	
	at 4.2 k	at 77 k
C_{11}	109.7 GPa	107.7 GPa
$(C_{11} - 2C_{12})/2$	28.4 GPa	28.0 GPa
C_{44}	19.0 GPa	18.7 GPa
$C_B = (C_{11} + 2C_{12})/3$	71.8 GPa	70.4 GPa
$\gamma_p = C_{12}/(C_{11} + C_{12})$	0.325	0.324

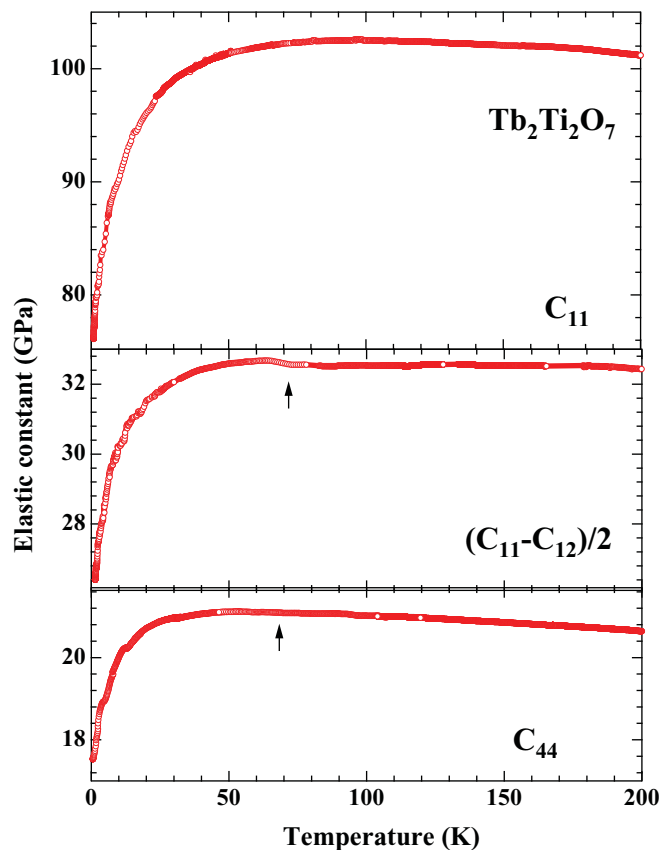


FIG. 3. (Color online) Temperature dependence of the elastic constants C_{11} , $(C_{11} - C_{12})/2$, and C_{44} of $\text{Tb}_2\text{Ti}_2\text{O}_7$. The anomaly is indicated by the arrows.

along the $\langle 100 \rangle$ axis, offset for clarity in ascending order from bottom to top. The arrows indicate the transition temperature point deduced from the phase diagram reported previously.^{25,26} The phase diagram was made using the specific heat and magnetic susceptibility measurements. A less distinct anomaly was observed at the boundary crossing, probably suggesting the transition to be of magnetic origin. The softening below 30 K becomes suppressed gradually with increasing magnetic field. These characteristic behaviors will be discussed below in detail, based on the degeneracy of quadrupolar degrees of freedom in the $4f$ -localized electronic ground state formed by the CEF effect.

TABLE III. The absolute values of each elastic constant and bulk modulus $C_B = (C_{11} + 2C_{12})/3$ and the Poisson ratio $\gamma_p = C_{12}/(C_{11} + C_{12})$ of $\text{Tb}_2\text{Ti}_2\text{O}_7$ at both 77 and 4.2 K.

Mode	Elastic constants	
	at 4.2 k	at 77 k
C_{11}	84.0 GPa	102.4 GPa
$(C_{11} - 2C_{12})/2$	28.1 GPa	32.6 GPa
C_{44}	18.9 GPa	21.1 GPa
$C_B = (C_{11} + 2C_{12})/3$	46.5 GPa	58.9 GPa
$\gamma_p = C_{12}/(C_{11} + C_{12})$	0.249	0.241

V. ANALYSIS AND DISCUSSION

First, let us discuss the elastic anomalies showing up at low temperatures. The pronounced elastic softening toward low temperature, observed in the temperature dependence of C_{11} , can be related to the $4f$ ground-state split by the CEF effect. Here, we consider the CEF splitting of the $4f$ level of R^{3+} in $R_2\text{Ti}_2\text{O}_7$. In the $R_2\text{Ti}_2\text{O}_7$ compounds, the R ions are at sites having trigonal symmetry D_{3d} . Under the crystalline electric field with this symmetry, the $4f$ multiplet 5I_8 of Ho^{3+} ($J = 8$) split down into five singlets and six doublets: $^5I_8 \rightarrow 3\Gamma_1 + 2\Gamma_2 + 6\Gamma_3$. And the $4f$ multiplet $^6H_{15/2}$ of Dy^{3+} ($J = 15/2$) split down into eight Kramers doublets. Finally, the $4f$ multiplet 7F_6 of Tb^{3+} ($J = 6$) split down into five singlets and four doublets: $^7F_6 \rightarrow 3\Gamma_1 + 2\Gamma_2 + 4\Gamma_3$. The Hamiltonian for the crystalline electric field interaction H_{CEF} of the trigonal symmetry D_{3d} of the R^{3+} ion is given by²⁷

$$H_{\text{CEF}} = B_2^0 O_2^0 + B_4^0 O_4^0 + B_4^3 O_4^3 + B_6^0 O_6^0 + B_6^3 O_6^3 + B_6^6 O_6^6. \quad (4)$$

Here, O_l^m are the Stevens equivalent operators expressed by the angular momentum J_x, J_y, J_z and B_k^m are the crystalline field parameters. In the case of a small trigonal distortion of the local cubic symmetry, the above Hamiltonian can be rewritten by the Hamiltonian

$$H_{\text{CEF}} = H_{\text{cub}} + B_2^0 O_2^0, \quad (5)$$

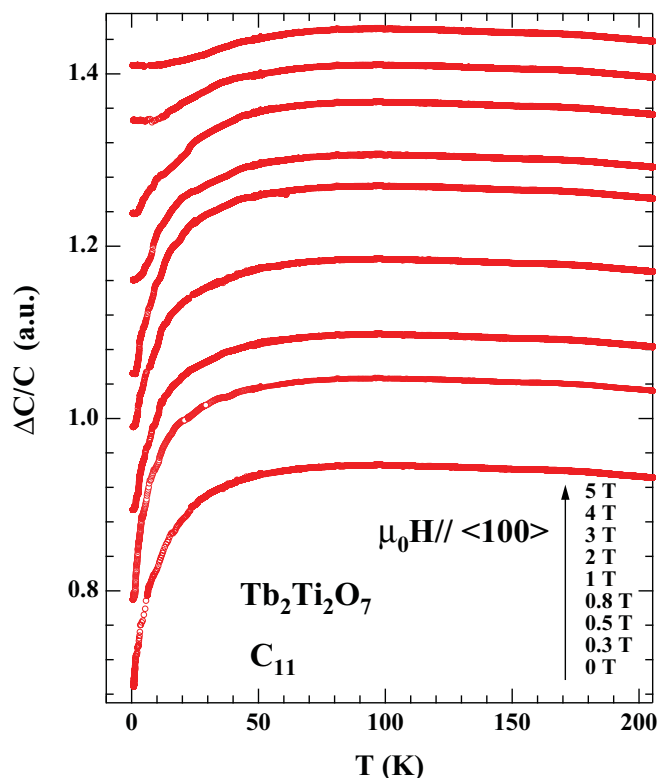


FIG. 4. (Color online) Temperature dependence of the elastic constants C_{11} of $\text{Tb}_2\text{Ti}_2\text{O}_7$ under the selected magnetic fields along the $\langle 100 \rangle$ axis, offset for clarity in ascending order from bottom to top.

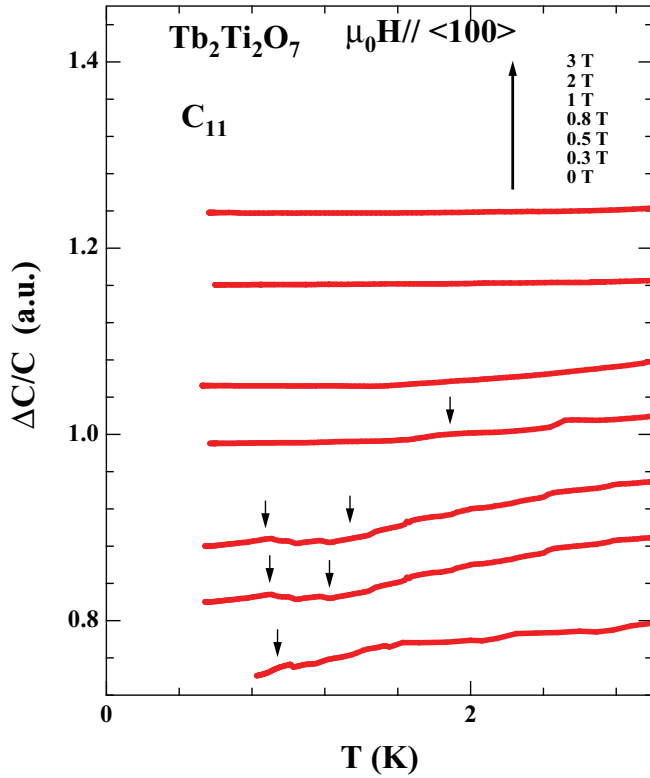


FIG. 5. (Color online) Low-temperature part of the elastic constants C_{11} of $\text{Tb}_2\text{Ti}_2\text{O}_7$ as a function of temperature under selected magnetic fields along the $\langle 100 \rangle$ axis, offset for clarity in ascending order from bottom to top. The arrows indicate a transition temperature deduced from the phase diagram reported previously.

where

$$H_{\text{cub}} = B_4^0(O_2^0 + 20\sqrt{2}O_4^3) + B_6\left({}^0O_6^0 - \frac{35}{2\sqrt{2}}O_6^3 + \frac{77}{8}O_6^6\right). \quad (6)$$

The quadrupolar susceptibility is calculated by the formula

$$\chi_{\Gamma}^{(s)}(T) = \sum_{ik} \frac{\exp(-E_{ik}^{(0)}/k_B T)}{Z} \frac{1}{k_B T} |\langle ik | O_{\Gamma} | ik \rangle|^2 - 2 \sum_{jl} \frac{|\langle ik | O_{\Gamma} | jl \rangle|^2}{E_i - E_j}, \quad (7)$$

where $|ik\rangle$ represents the k th eigenfunction of the i th CEF level. When the ground state or the low-lying states are degenerate with respect to the quadrupolar moment O_{Γ} , a softening in the corresponding elastic constant is expected to occur due to the nonzero Curie term, which is proportional to the inverse temperature. Thus, absence of the softening indicates that the ground state of R^{3+} is not degenerate with respect to the quadrupolar moment O_{Γ} or the ground state would be isolated well in the CEF level scheme in $\text{Dy}_2\text{Ti}_2\text{O}_7$ and $\text{Ho}_2\text{Ti}_2\text{O}_7$. In fact, inelastic neutron scattering measurements on $\text{Ho}_2\text{Ti}_2\text{O}_7$ indicate that the ground state of Ho^{3+} is an almost pure $|J, J_z\rangle \approx |8, \pm 8\rangle$ doublet, well separated from the first excited state at 236.6 K.²⁸ Furthermore, analysis of the temperature dependencies of the susceptibility

and the field dependencies of the magnetization indicates that the ground state of Dy^{3+} is an almost pure $|J, J_z\rangle \approx |15/2, \pm 15/2\rangle$ doublet with a slight admixture of states with other J_z , also well separated from the first excited state at 150 K.^{29,30}

On the other hand, the ground state of Tb^{3+} in $\text{Tb}_2\text{Ti}_2\text{O}_7$ differs considerably from that in the $\text{Dy}_2\text{Ti}_2\text{O}_7$ and $\text{Ho}_2\text{Ti}_2\text{O}_7$ compounds. $\text{Tb}_2\text{Ti}_2\text{O}_7$ shows the first excited level at around 16 K, forming a strong admixture to the ground state in the magnetic field. Previous studies suggested that the ground state is a non-Kramers doublet $0.747 |\pm 5\rangle - 0.665 |\mp 1\rangle$ with a nearby non-Kramers doublet $0.816 |\pm 4\rangle - 0.577 |\mp 2\rangle$ at energy distances of 16 K.²⁷⁻²⁹ Thus, from the present results we can conclude that a significant difference of the low-lying CEF levels leads to such a pronounced elastic softening toward low temperature in $\text{Tb}_2\text{Ti}_2\text{O}_7$, whereas no elastic softening was observed in $\text{Dy}_2\text{Ti}_2\text{O}_7$ and $\text{Ho}_2\text{Ti}_2\text{O}_7$.

We analyzed the elastic softening showing up in $\text{Tb}_2\text{Ti}_2\text{O}_7$ based on Eqs. (3) and (7). The fitting results are shown by the solid lines in Fig. 6. The previously proposed CEF levels can fit the experimental data reasonably. The fitting

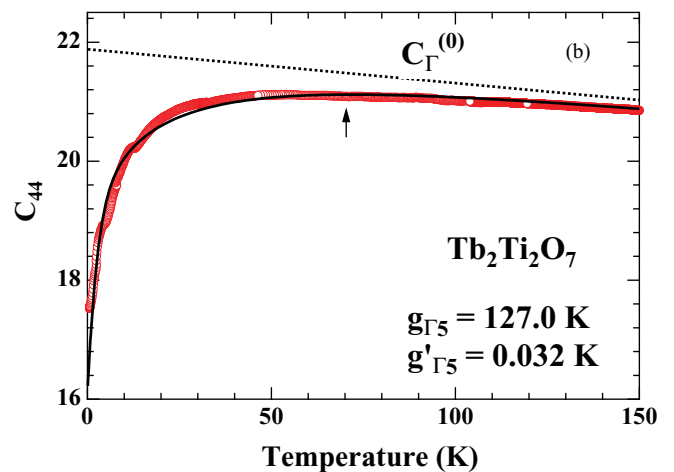
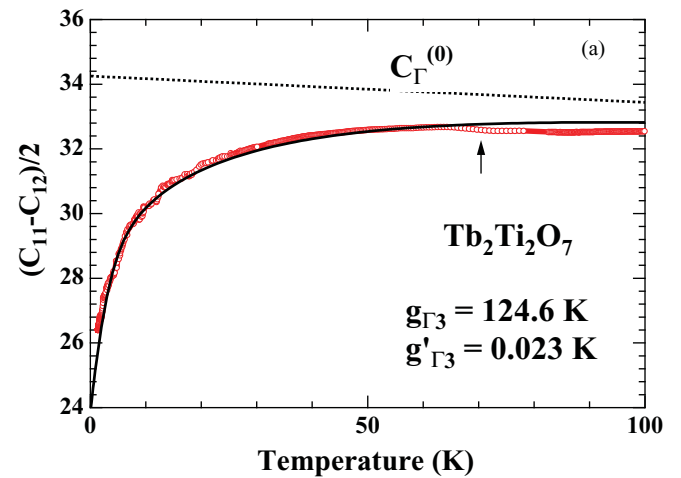


FIG. 6. (Color online) Temperature dependence of the elastic constant $(C_{11} - C_{12})/2$ below 100 K (a) and C_{44} below 150 K (b) with the calculated result based on Eq. (3). The anomaly is indicated by the arrows.

curves as shown in Fig. 6 give us important microscopic parameters of $\text{Tb}_2\text{Ti}_2\text{O}_7$ such as quadrupolar coupling and intersite quadrupolar interaction constants as follows: $g'_{\Gamma_3} = 23$ mK and $g_{\Gamma_3} = 124.6$ K for $(C_{11} - C_{12})/2$ in Fig. 6(a) and $g'_{\Gamma_5} = 32$ mK and $g_{\Gamma_5} = 127.0$ K for C_{44} in Fig. 6(b). They should be compared with those for TmTe and for $\text{Ce}_3\text{Pd}_{20}\text{Ge}_6$, which undergo a quadrupolar transition at 1.8 and 1.3 K, respectively.^{31,32} The parameters for TmTe were $g'_{\Gamma_3} = -250$ mK, $g_{\Gamma_3} = 63$ K, $g'_{\Gamma_5} = -76$ mK, and $g_{\Gamma_5} = 81$ K, and for $\text{Ce}_3\text{Pd}_{20}\text{Ge}_6$ they were $g'_{\Gamma_3} = 10$ mK, $g_{\Gamma_3} = 107$ K, $g'_{\Gamma_5} = 190$ mK, and $g_{\Gamma_5} = 89$ K. Although the value of g for $\text{Tb}_2\text{Ti}_2\text{O}_7$ is larger than those for TmTe and for $\text{Ce}_3\text{Pd}_{20}\text{Ge}_6$, the value of g' for $\text{Tb}_2\text{Ti}_2\text{O}_7$ is fairly small compared to those for TmTe and for $\text{Ce}_3\text{Pd}_{20}\text{Ge}_6$. It would be better to say that the intersite quadrupolar interaction g' of this system is fairly suppressed compared to that for other typical rare-earth compounds. This suppression would be due to the geometrical frustration derived from the characteristic pyrochlore crystal structure. We naively suggest that these observations point to the possibility that the quadrupolar degrees of freedom formed by the ground and low-lying states is playing an essential role in the giant magnetostriction values in $\text{Tb}_2\text{Ti}_2\text{O}_7$ at low temperatures. Furthermore, the intersite quadrupolar interaction mediated among quadrupolar moments would be suppressed strongly by the three-dimensional geometrically frustrated situation, leading to the absence of quadrupolar ordering. Since the coupling constant g_{Γ} between elastic strains and quadrupolar moments is substantial, alignment of the quadrupolar moments by applying a magnetic field via a spin-orbital L - S coupling would cause significant elastic strictions, including the so-called exchange striction in $\text{Tb}_2\text{Ti}_2\text{O}_7$. In this study, it was found that the elastic constants, which are closely related to magnetostriction, are huge and considerably affected by application of a magnetic field in $\text{Tb}_2\text{Ti}_2\text{O}_7$. This experimental fact strongly indicates that the orbital degrees of freedom derived from Tb ions play a crucial role in giant magnetoresistance.

Finally, we would like to comment on the possible transition in $\text{Dy}_2\text{Ti}_2\text{O}_7$ and $\text{Ho}_2\text{Ti}_2\text{O}_7$. A smooth anomaly was observed in the temperature dependence of the elastic constants at around 80 K in $\text{Dy}_2\text{Ti}_2\text{O}_7$, $\text{Ho}_2\text{Ti}_2\text{O}_7$, and $\text{Tb}_2\text{Ti}_2\text{O}_7$ as well. Even in $\text{Tb}_2\text{Ti}_2\text{O}_7$, a slight anomaly can be detected, as shown in Fig. 3. This anomaly was also confirmed by the temperature dependence of the permittivities $\varepsilon(T)$ and loss-angle tangent, $\tan\delta$, and a distinct softening in Raman spectra.^{24,33,34} A characteristic anomaly was observed in the temperature dependencies of the relative permittivities $\varepsilon(T)$ and of the $\tan\delta$ obtained for $\text{Dy}_2\text{Ti}_2\text{O}_7$ and $\text{Ho}_2\text{Ti}_2\text{O}_7$. Namely, a clear dip was observed in $\varepsilon(T)$ being accompanied by a sharp maximum in $\tan\delta$ - T . However, microscopic measurements and lattice parameters did not show any evidence to confirm this anomaly. Thus, no ferroelectric or other structural phase transitions occur at a temperature of 80 K in either com-

pound. A local distortion without a structural phase transition might occur, resulting in superlattice formation. Actually, the presence of two inequivalent Tb^{3+} sites is suggested in the low-temperature structure in Raman spectroscopy.³⁴ As far as we know, $\text{Dy}_2\text{Ti}_2\text{O}_7$ and $\text{Ho}_2\text{Ti}_2\text{O}_7$ are the only systems which exhibit this anomaly in the temperature dependence of elastic constants and permittivities in the α -pyrochlore spin compounds. The origin of the elastic anomaly showing up in the temperature dependence of C_{Γ} around 120 K in $\text{Dy}_2\text{Ti}_2\text{O}_7$ and $\text{Ho}_2\text{Ti}_2\text{O}_7$ is still an open issue to be solved. However, this physical implication may involve a proper treatment of the symmetry of the crystal structure. A significantly small distortion or/and symmetry breaking may occur in the α -pyrochlore crystal structure. Experimental confirmation is highly desired.

VI. CONCLUDING REMARKS

The high quality and large size of single crystals and high-resolution ultrasonic measurements allowed us to explore the peculiar features in the elastic properties of the α -pyrochlore spin compounds $R_2\text{Ti}_2\text{O}_7$, $R = \text{Tb}, \text{Dy},$ and Ho . The obtained data confirm an important role of the CEF level scheme in the pronounced giant magnetoelastic effect. For $\text{Tb}_2\text{Ti}_2\text{O}_7$ large softening toward low temperature was observed in the temperature dependence of elastic constants. From the pronounced softening, we estimated important microscopic parameters such as quadrupolar coupling and intersite quadrupolar interaction constants. The values would be large enough to bring about a quadrupolar ordering. This suggests that the geometrically structural frustration would suppress the formation of the long-range ordering. Although the microscopic origin of the lattice anomaly showing up at around 80 K in $R_2\text{Ti}_2\text{O}_7$ ($R = \text{Dy}, \text{Ho},$ and probably Tb) still remains to be investigated, we believe this finding provides an important key for forming the geometrically structural frustration in the α -pyrochlore spin compounds $R_2\text{Ti}_2\text{O}_7$. The microscopic details of each atomic displacement in $R_2\text{Ti}_2\text{O}_7$ below and above this temperature will be understood fully after detailed experiments such as x-ray and nuclear magnetic resonance measurements.

ACKNOWLEDGMENTS

Y.N. and M.Y. are grateful to M. Nakamura for his help in the operation of the cryogenic apparatus. The measurements have been performed in the Cryogenic Division of the Center for Instrumental Analysis, Iwate University. This work was supported by a Grant-in-Aid for Scientific Research on Priority Areas "Novel States of Matter Induced by Frustration" (No. 19052005).

*yoshiki@iwate-u.ac.jp

¹See, for example, S. T. Bramwell and M. J. P. Gingras, *Science* **294**, 1495 (2001).

²L. H. Brixner, *Inorg. Chem.* **3**, 1065 (1964).

³M. J. Harris, S. T. Bramwell, D. F. McMorrow, T. Zeiske, and K. W. Godfrey, *Phys. Rev. Lett.* **79**, 2554 (1997).

- ⁴B. C. den Hertog and M. J. P. Gingras, *Phys. Rev. Lett.* **84**, 3430 (2000).
- ⁵K. Matsuhira, Y. Hinatsu, K. Tenya, and T. Sakakibara, *J. Phys. Condens. Matter* **12**, L649 (2000).
- ⁶K. Matsuhira, Y. Hinatsu, and T. Sakakibara, *J. Phys. Condens. Matter* **13**, L737 (2001).
- ⁷K. Matsuhira, Z. Hiroi, T. Tayama, S. Takagi, and T. Sakakibara, *J. Phys. Condens. Matter* **14**, L559 (2002).
- ⁸T. Sakakibara, T. Tayama, Z. Hiroi, K. Matsuhira, and S. Takagi, *Phys. Rev. Lett.* **90**, 207205 (2003).
- ⁹N. Hamaguchi, T. Matsushita, N. Wada, Y. Yasui, and M. Sato, *Phys. Rev. B* **69**, 132413 (2004).
- ¹⁰H. Fukazawa, R. G. Melko, R. Higashinaka, Y. Maeno, and M. J. P. Gingras, *Phys. Rev. B* **65**, 054410 (2002).
- ¹¹R. Higashinaka, H. Fukazawa, and Y. Maeno, *Phys. Rev. B* **68**, 014415 (2003).
- ¹²J. S. Gardner, S. R. Dunsiger, B. D. Gaulin, M. J. P. Gingras, J. E. Greedan, R. F. Kiefl, M. D. Lumsden, W. A. MacFarlane, N. P. Raju, J. E. Sonier, I. Swainson, and Z. Tun, *Phys. Rev. Lett.* **82**, 1012 (1999).
- ¹³M. Kanada, Y. Yasui, M. Ito, H. Harashina, M. Sato, H. Okumura, and K. Kakurai, *J. Phys. Soc. Jpn.* **68**, 3802 (1999).
- ¹⁴J. P. C. Ruff, B. D. Gaulin, J. P. Castellán, K. C. Rule, J. P. Clancy, J. Rodriguez, and H. A. Dabkowska, *Phys. Rev. Lett.* **99**, 237202 (2007).
- ¹⁵A. P. Ramirez, A. Hayashi, R. J. Cava, R. Siddharthan, and B. S. Shastry, *Nature (London)* **399**, 333 (1999).
- ¹⁶P. M. Levy, *J. Phys. C* **6**, 3545 (1973).
- ¹⁷M. E. Mullen, B. Lüthi, P. S. Wang, E. Bucher, L. D. Longinotti, J. P. Maita, and H. R. Ott, *Phys. Rev. B* **10**, 186 (1974).
- ¹⁸V. Dohm and P. Fulde, *Z. Phys. B* **21**, 369 (1975).
- ¹⁹B. Lüthi, *J. Magn. Magn. Mater.* **52**, 70 (1985).
- ²⁰P. Thalmeier, *J. Magn. Magn. Mater.* **76&77**, 299 (1988).
- ²¹S. Nakamura, T. Goto, Y. Ishikawa, S. Sakatsume, and M. Kasuya, *J. Phys. Soc. Jpn.* **60**, 2305 (1991).
- ²²S. Nakamura, T. Goto, M. Kasaya, and S. Kunii, *J. Phys. Soc. Jpn.* **60**, 4311 (1991).
- ²³S. Nakamura, T. Goto, Y. Ishikawa, S. Sakatsume, and M. Kasuya, *J. Phys. Soc. Jpn.* **63**, 623 (1994).
- ²⁴L. G. Mamsurova, K. S. Pigal'skiĭ, N. G. Trusevich, and L. G. Shcherbakova, *Sov. Phys. Solid State* **27**, 978 (1985).
- ²⁵N. Hamaguchi, T. Matsushita, N. Wada, Y. Yasui, and M. Sato, *J. Magn. Magn. Mater.* **272–276**, E1007 (2004).
- ²⁶N. Hamaguchi, T. Matsushita, N. Wada, Y. Yasui, and M. Sato, *Phys. Rev. B* **69**, 132413 (2004).
- ²⁷I. V. Aleksandrov, B. V. Lidskiĭ, L. G. Mamsurova, M. G. Neĭgauz, K. S. Pigal'skiĭ, K. K. Pukhov, N. G. Trusevich, and L. G. Shcherbakova, *Sov. Phys. JETP* **62**, 1287 (1985).
- ²⁸S. Rosenkranz, A. P. Ramirez, A. Hayashi, R. J. Cava, R. Siddharthan, and B. S. Shastry, *J. Appl. Phys.* **87**, 5914 (2000).
- ²⁹L. G. Mamsurova, K. K. Pukhov, N. G. Trusevich, and L. G. Shcherbakova, *Sov. Phys. Solid State* **27**, 1214 (1985).
- ³⁰L. G. Mamsurova, K. S. Pigal'skiĭ, K. K. Pukhov, N. G. Trusevich, and L. G. Shcherbakova, *Sov. Phys. JETP* **67**, 550 (1988).
- ³¹T. Matsumura, S. Nakamura, T. Goto, H. Amitsuka, K. Matsuhira, T. Sakakibara, and T. Suzuki, *J. Phys. Soc. Jpn.* **67**, 612 (1998).
- ³²Y. Nemoto, T. Yamaguchi, T. Horino, M. Akatsu, T. Yanagisawa, and T. Goto, *Phys. Rev. B* **68**, 184109 (2003).
- ³³M. Maczka, M. L. Sanjuan, A. F. Fuentes, K. Hermanowicz, and J. Hanuza, *Phys. Rev. B* **78**, 134420 (2008).
- ³⁴T. T. A. Lummen, I. P. Handayani, M. C. Donker, D. Fausti, G. Dhahlenne, P. Berthet, A. Revcolevschi, and P. H. M. van Loosdrecht, *Phys. Rev. B* **77**, 214310 (2008).